Hindawi
Mathematical Problems in Engineering
Volume 2019, Article ID 6095184, 13 pages
https://doi.org/10.1155/2019/6095184

Research Article

Dynamic Force Identification Problem Based on a Novel Improved Tikhonov Regularization Method

Chunping Ren[1], **Nengjian Wang**[1], **Qinhui Liu**[1], **and Chunsheng Liu**[2]

[1] *College of Mechanical and Electrical Engineering, Harbin Engineering University, Harbin 150001, China*
[2] *Heilongjiang University of Science and Technology, Harbin 150022, China*

Correspondence should be addressed to Chunping Ren; renchunpin@sina.com and Qinhui Liu; liuqinhui@hrbeu.edu.cn

Received 17 January 2019; Revised 6 March 2019; Accepted 12 March 2019; Published 2 April 2019

Academic Editor: Łukasz Jankowski

The main purpose of this paper is to identify the dynamic forces between the conical pick and the coal-seam. According to the theory of time domain method, the dynamic force identification problem of the system is established. The direct problem is described by Green kernel function method. The dynamic force is expressed by a series of functions superposed by impulses, and the dynamic response of the structure is expressed as a convolution integral form between the input dynamic force and the response of Green kernel function. Because of the ill-conditioned characteristics of the structure matrix and the influence of measurement noise in the process of dynamic force identification, it is difficult to deal with this problem by the usual numerical method. In present content, a novel improved Tikhonov regularization method is proposed to solve ill-posed problems. An engineering example shows that the proposed method is effective and can obtain stable approximate solutions to meet the engineering requirements.

1. Introduction

Various mechanical and electrical products are often subjected to a variety of dynamic loads, including vibration, impact, noise, and thermal environment [1]. It is important for the safety and accurate design of structures to accurately determine these loads. In many cases, it is difficult to directly measure the external loads of large structures such as missiles, aircraft, and offshore platforms under the action of wind waves or alternating excitations. Dynamic load identification is based on the dynamic response of the measured system and the known dynamic characteristics of the system to solve the dynamic loads on the structure. In practical engineering, it is very difficult to directly measure dynamic loads. Therefore, load identification is an indirect method to obtain the required load [2–4].

At present, load identification methods mainly include frequency domain method and time domain method [5–7]. Frequency domain method was put forward earlier. Its basic idea is to identify excitation spectrum by response spectrum. It is mainly realized by inversion of frequency response function between excitation and response. However, the ill-conditioned problem of coefficient matrix and singular value decomposition problem are often encountered in matrix inversion [8–10]. Based on the back analysis of the complex convolution relationship between load and response, the time domain method directly determines the time history of dynamic force, which has a good application prospect in engineering. For instance, [11] adopted the singular value decomposition (SVD) method to predict hourly load and peak load for the next selected time span. Reference [12] presented a new approach for solving specific classes of inverse source identification problems. Reference [13] used a modified inverse patch transfer function (IPTF) method to reconstruct the normal velocities of the target source in a noisy environment, and [14] used neural network in combination with genetic programming to implement the load identification of electric equipment. Reference [15] proposed the finite element and wavelet-based method for reconstructing the moving force. In [16], a new and effective algorithm for optimization problems, GPSA, is utilized in civil engineering. Reference [17] presented a single-point method for the identification of prevailing disturbing loads in power systems. But we may encounter some difficulties.

It is very difficult to use the above methods for large-scale and complex load identification problems. Meanwhile, in practical engineering problems, it is necessary to identify the random dynamic force on pick and coal-seam structure. Unfortunately, they are complex inverse problems with inherent ill-posedness.

Fortunately, there are many popular regularization methods to deal with the ill-posed problem in practical engineering applications [18–22]. It is well known that the Tikhonov regularization method [23], as a traditional technique, has been widely used in various mathematical and engineering problems to deal with ill-posedness [24], for instance, parameter reconstruction, force source reconstruction problem, and so on [25–29]. Reference [30] applied the Tikhonov regularization method to reconstruct the dynamic force. Reference [31] demonstrated that the Tikhonov regularization method can solve the inverse problem in a stable manner despite the presence of noisy data. Reference [32] identified the shock load on an electroelastic bimorph disk using the Tikhonov regularization method. However, the Tikhonov regularization method is not completely perfect; there are numerous unavoidable limitations and disadvantages, which is described as follows: (a) the approximate solution provided by Tikhonov regularization method is too smooth; (b) the approximate solution provided by Tikhonov regularization method may lack some details that the desired real solution might possess. Therefore, it is very necessary to discuss other regularization methods to improve the limitations and disadvantages of the regularization method mentioned above.

Considering the limitations of the above methods in a certain case, we propose a novel improved Tikhonov regularization method to offer a stable solution for the ill-posed problems in practical engineering applications. Compared with the conventional methods, the uniqueness and improvement of the proposed method are obtained in this paper.

First and foremost, the paper is different from the conventional methods, and the uniqueness and improvement of this paper can be described as follows: (a) a novel improved Tikhonov regularization method can make the error of the regularization solution reach the asymptotic optimal order; (b) a novel improved Tikhonov regularization method has better convergence, and the detailed information of the solution is clearly enhanced; (c) the method we propose can effectively overcome the smoothness of the solution of the ill-posed problem; (d) the proposed method not only eliminates the influence of large singular values but also ensures the filtering of small singular values; (e) the small perturbation of right-end data will not affect the accuracy of inversion results, which fully reflects the good stability of the improved method.

In this study, our main purpose is to effectively identify the dynamic force between conical pick and coal-seam by using a novel improved Tikhonov regularization method. The rest of this study is structured as follows. In Section 2, the inverse problem model is established. In Section 3, a novel improved Tikhonov regularization method is proposed. In Section 4, the stability of the proposed method is proved. In Section 5, an engineering application example is discussed. Some valuable conclusions are described in Section 6.

2. Establishment of Inverse Problem Model

The inverse problems encountered in engineering can be expressed by the following [33, 34]:

$$y(t) = \int_0^t k(t-\tau)\, x(\tau)\, d\tau, \quad (1)$$

where y(t) is the response which can be displacement, velocity, acceleration, strain, etc. k(t) is the corresponding Green's function that is the kernel of impulse response. x(t) is the identified dynamic force.

Using the rectangular formula, we can get the discrete form of (1).

$$\sum_{i=1}^{n} \mathrm{k}(t_k - \tau_i)\, \mathrm{x}(\tau_i)\, \Delta \mathrm{T} = \mathrm{y}(t_i). \quad (2)$$

where ΔT denotes the time interval and it can be rewritten as follows:

$$\mathrm{x}_i = \mathrm{x}(\tau_i), \quad (3)$$

$$\mathrm{y}_i = \mathrm{y}(t_i), \quad (4)$$

$$\mathrm{k}_{k-i} = \mathrm{k}(t_k - \tau_i). \quad (5)$$

So

$$\mathbf{X} = (\mathrm{x}_1, \mathrm{x}_2, \mathrm{x}_3, \cdots \mathrm{x}_n)^{\mathrm{T}}, \quad (6)$$

$$\mathbf{Y} = (y_1, \mathrm{y}_2, \mathrm{y}_3, \cdots \mathrm{y}_n)^{\mathrm{T}}, \quad (7)$$

$$\mathbf{K} = (\mathrm{k}_{k-i})\, \Delta \mathrm{T}. \quad (8)$$

Hence, (2) can be simply written as

$$\mathbf{Y}(t) = \mathbf{K}(t)\, \mathbf{X}(t), \quad (9)$$

or equivalently,

$$\begin{pmatrix} y_1 \\ y_2 \\ \vdots \\ y_m \end{pmatrix} = \begin{pmatrix} k_1 & & & \\ k_2 & k_1 & & \\ \vdots & \vdots & \ddots & \\ k_m & k_{m-1} & \dots & k_1 \end{pmatrix} \begin{pmatrix} x_1 \\ x_2 \\ \vdots \\ x_m \end{pmatrix} \Delta t, \quad (10)$$

Where y_i, k_i, and x_i denote structural dynamic response, Green's function matrix, and input force at time $t = i\Delta t$, respectively.

Because the condition number of K is very large and the response signal Y measured in practice always contains noise, a very small disturbance can result in a huge solution deviation. So dynamic force identification is a typical ill-conditioned problem, and it is inappropriate to directly invert K in (3).

The above characteristics of ill-conditioned problems do not mean that ill-conditioned problems are not solvable but that traditional linear algebraic methods cannot be directly applied to solve such problems.

Therefore, in order to make the solution meaningful, the approximate solution is usually obtained by regularization technique.

3. The Regularization Method for Solving Inverse Problem

3.1. Preliminaries. As we all know, we have the following lemma for regularized filter functions.

Lemma 1 (see [35]). *Let X and Y be Hilbert spaces, $K: X \longrightarrow Y$ be a compact operator, (μ_i, x_i, y_i) be a singular system for the linear operator $K: X \longrightarrow Y$, and the function q be defined: $(0,+\infty)\times(0,\|K\|] \longrightarrow R$; then we have the following properties:*

$$\left|q(\alpha,\mu)\right| \leq 1, \quad \forall\alpha\,(0,+\infty),\ \forall\mu \in (0,\|K\|). \tag{11}$$

$\forall\alpha(0,+\infty)$, there is a constant $c(\alpha) > 0$, such that $|q(\alpha,\mu)| \leq c(\alpha)\mu$ and $\forall\mu \in (0,\|K\|)$;

$$\lim_{\alpha\longrightarrow 0} q(\alpha,\mu) = 1, \quad \forall\mu \in (0,\|K\|). \tag{12}$$

Operator $R_\alpha: Y \longrightarrow X$ is defined by the following formula:

$$R_\alpha y = \sum_{i=1}^{\infty} \frac{q(\alpha,\mu_i)}{\mu_i}(y, y_i)\, x_i. \tag{13}$$

which is a regularization method, and $\|R_\alpha\| \leq c(\alpha)$.

The function $q(\alpha,\mu)$ with the above properties is called a regularized filter function of K.

For the famous Tikhonov regularization method, the Tikhonov regularization solution is the minimum value of Tikhonov functional; a singular system with compact operators can be expressed as

$$x_\alpha^\delta = R_\alpha y_\delta = \sum_{i=1}^{\infty} \frac{q(\alpha,\mu_i)}{\mu_i}(y_\delta, y_i)\, x_i. \tag{14}$$

$q(\alpha,\mu)$ is the Tikhonov regularized filter function, and $q(\alpha,\mu) = \mu^2/(\alpha+\mu^2)$, $\alpha > 0$, $0 < \mu \leq \|K\|$. Next, we will get a new regularization method by giving a new regularization filter function.

3.2. A Novel Improved Tikhonov Regularization Method. According to the regularization theory, the regularization operator R_α can be constructed by regularization filter function $q(\alpha,\mu)$, which provides a theoretical basis for establishing a new regularization method.

In this paper, a novel improved regularized filter function is constructed as follows:

$$q(\alpha,\mu) = \begin{cases} 1 & \mu^{\sigma r} \geq \alpha \\ \dfrac{\mu^\sigma}{(\alpha+\mu^{\sigma r})^{1/r}} & \mu^{\sigma r} < \alpha \end{cases} \tag{15}$$

where $\alpha > 0$, $0 < \mu \leq \|K\|$, and $r > 0$, $\sigma \geq 1$.

The method proposed in this paper can not only ensure that the large singular values are not corrected but also filter the small singular values without affecting the accuracy of the solutions.

Theorem 2. *The function $q(\alpha,\mu)$ defined by formula (8) is a kind of regularized filter function.*

Proof. ① When $\mu^{\sigma r} \geq \alpha$, $q(\alpha,\mu) = 1 \leq 1$;

when $\mu^{\sigma r} < \alpha$, we all know

$$\mu^\sigma = \left(\mu^{\sigma r}\right)^{1/r} < \left(\alpha+\mu^{\sigma r}\right)^{1/r} \tag{16}$$

Therefore, we get

$$q(\alpha,\mu) = \frac{\mu^\sigma}{(\alpha+\mu^{\sigma r})^{1/r}} < 1. \tag{17}$$

② When $\mu^{\sigma r} \geq \alpha$, $\mu^{\sigma r}/\alpha \geq 1 \Longrightarrow \mu/\alpha^{1/\sigma r} \geq 1$, such that

$$q(\alpha,\mu) = 1 \leq \frac{1}{\alpha^{1/\sigma r}}\cdot\mu; \tag{18}$$

when $\mu^{\sigma r} < \alpha$, $q(\alpha,\mu) = \mu^\sigma/(\alpha+\mu^{\sigma r})^{1/r}$.

When $\sigma = 1$, we have

$$q(\alpha,\mu) = \frac{\mu}{(\alpha+\mu^r)^{1/r}} \leq \frac{\mu}{\alpha^{1/r}}. \tag{19}$$

When $\sigma > 1$, $\alpha+\mu^{\sigma r} \geq \alpha^{1/p}\cdot\mu^{\sigma r/q}$.

Letting $p = \sigma$, $q = \sigma/(\sigma-1)$, we have

$$\alpha+\mu^{\sigma r} \geq \alpha^{1/\sigma}\cdot\mu^{r(\sigma-1)}. \tag{20}$$

Then

$$\left(\alpha+\mu^{\sigma r}\right)^{1/r} \geq \alpha^{1/\sigma r}\cdot\mu^{\sigma-1}, \tag{21}$$

such that

$$\frac{\mu^\sigma}{(\alpha+\mu^{\sigma r})^{1/r}} \leq \frac{\mu^\sigma}{\alpha^{1/r\sigma}\cdot\mu^{\sigma-1}} = \frac{\mu}{\alpha^{1/r\sigma}}. \tag{22}$$

Hence, $\forall\sigma \geq 1$, we have $q(\alpha,\mu) = \mu/\alpha^{1/\sigma r}$.

And $\forall \alpha > 0$; we can obtain

$$|q(\alpha,\mu)| = \frac{1}{\alpha^{1/\sigma r}} \cdot \mu = c(\alpha)\mu. \tag{23}$$

③ When $\alpha \longrightarrow 0$, $q(\alpha, \mu) = 1$.

It is known from Theorem 2

$$q(\alpha,\mu) = \begin{cases} 1 & \mu^{\sigma r} \geq \alpha \\ \dfrac{\mu^{\sigma}}{(\alpha + \mu^{\sigma r})^{1/r}} & \mu^{\sigma r} < \alpha \end{cases} \tag{24}$$

which is a kind of regularized filter functions and its corresponding regularization operator is $R_\alpha : Y \longrightarrow X$

$$R_\alpha y = \sum_{i=1}^{\infty} \frac{q(\alpha,\mu_i)}{\mu_i}(y, y_i)\, x_i. \tag{25}$$

In order to express the advanced filtering operator of the proposed method more clearly, we give another representation of its filtering algorithm.

Substituting formula (13) into formula (14), we can get

$$\begin{aligned} R_\alpha y &= \sum_{i=1}^{k} \frac{1}{\mu}(y, y_i)\, x_i \\ &+ \sum_{i=k+1}^{\infty} \frac{1}{\mu_i} \cdot \frac{\mu_i^{\beta}}{\left(\alpha + \mu_i^{\beta i}\right)^{1/\gamma}}(y, y_i)\, x_i \end{aligned} \tag{26}$$

Introduce the singular value decomposition (SVD) [36]:

$$\mathrm{A} = \mathbf{U}\sum \mathbf{V}^{\mathrm{T}} = \sum_{i=1}^{n} u_i \sigma_i v_i^T, \tag{27}$$

in which $\mathbf{U} = (u_1, u_2, u_3, \cdots u_{n+1})$ and $\mathbf{V} = (v_1, v_2, v_3, \cdots v_{n+1})$ are orthogonal matrices and $\sum = \mathrm{diag}(\sigma_1, \sigma_2, \sigma_3, \cdots \sigma_{n+1})$.

$$\sigma_1 \geq \sigma_2 \geq \sigma_3 \geq \cdots \geq \sigma_n > \sigma_{n+1}. \tag{28}$$

Substituting formula (27) into formula (26), we can get

$$\begin{aligned} R_\alpha y &= \sum_{i=1}^{k} \frac{1}{\sigma_i}(y, u_i)\, v_i \\ &+ \sum_{i=k+1}^{n+1} \frac{1}{\sigma_i} \cdot \frac{\sigma_i^{\beta}}{\left(\alpha + \sigma_i^{\beta\gamma}\right)^{1/\gamma}}(y, u_i)\, v_i \\ &= \sum_{i=1}^{k} \frac{u_i^T y}{\sigma_i} v_i + \sum_{i=k+1}^{n+1} \left(\frac{\sigma_i^{\beta}}{\left(\alpha + \sigma_i^{\beta\gamma}\right)^{1/\gamma}} \right) \frac{u_i^T y}{\sigma_i} v_i \end{aligned} \tag{29}$$

Then, we have

$$\begin{aligned} R_\alpha y &= \frac{u_1^T y}{\sigma_1} v_1 + \frac{u_2^T y}{\sigma_2} v_2 + \cdots \frac{u_k^T y}{\sigma_k} v_k \\ &+ \frac{\sigma_{k+1}^{\beta}}{\left(\alpha + \sigma_{k+1}^{\beta\gamma}\right)^{1/\gamma}} \frac{u_{k+1}^T y}{\sigma_{k+1}} v_{k+1} \\ &+ \cdots \frac{\sigma_{n+1}^{\beta}}{\left(\alpha + \sigma_{n+1}^{\beta\gamma}\right)^{1/\gamma}} \frac{u_{n+1}^T y}{\sigma_{n+1}} v_{n+1} = [v_1, v_2 \cdots v_{n+1}] \\ &\begin{bmatrix} \frac{1}{\sigma_1} & & & & \\ & \ddots & & & \\ & & \frac{1}{\sigma_k} & & \\ & & & \ddots & \\ & & & & \frac{1}{\sigma_{k+1}} \cdot \frac{\sigma_{k+1}^{\beta}}{\left(\alpha + \sigma_{k+1}^{\beta\gamma}\right)^{1/\gamma}} \end{bmatrix} \cdot \begin{bmatrix} u_1^T \\ u_2^T \\ u_3^T \\ \vdots \\ u_{n+1}^T \end{bmatrix} \\ &\cdot y = [v_1, v_2 \cdots v_{n+1}] \cdot \\ &\begin{bmatrix} 1 & & & & \\ & \ddots & & & \\ & & 1 & & \\ & & & \ddots & \\ & & & & \frac{1}{\sigma_{k+1}} \cdot \frac{\sigma_{k+1}^{\beta}}{\left(\alpha + \sigma_{k+1}^{\beta\gamma}\right)^{1/\gamma}} \end{bmatrix} \\ &\cdot \begin{bmatrix} \sigma_1^{-1} & & & \\ & \sigma_2^{-1} & & \\ & & \ddots & \\ & & & \sigma_{n+1}^{-1} \end{bmatrix} \cdot \begin{bmatrix} u_1^T \\ u_2^T \\ u_3^T \\ \vdots \\ u_{n+1}^T \end{bmatrix} \cdot y = V \cdot M_{\beta,\gamma}^{\alpha} \\ &\cdot \sum^{-1} U y. \end{aligned} \tag{30}$$

in which

$$M_{\beta,\gamma}^{\alpha} = \begin{bmatrix} 1 & & & & \\ & \ddots & & & \\ & & 1 & & \\ & & & \ddots & \\ & & & & \frac{1}{\sigma_{k+1}} \cdot \frac{\sigma_{k+1}^{\beta}}{\left(\alpha + \sigma_{k+1}^{\beta\gamma}\right)^{1/\gamma}} \end{bmatrix} \tag{31}$$

Hence, we can have

$$R_\alpha = V \cdot M^{\alpha}_{\beta,\gamma} \cdot \sum^{-1} U. \quad (32)$$

Comparing the Tikhonov regularization method with the improved Tikhonov regularization method, according to formula (31), we can see that, in part $\sigma_i^{\beta\gamma} \geq \alpha$, change from $\sigma_i^2/(\alpha+\sigma_i^2)$ to 1, $1 \leq i \leq k$, this eliminates the effect of large singular values.

When $\sigma_i^{\beta\gamma} < \alpha$ change from $\sigma_i^2/(\alpha+\sigma_i^2)$ to $\sigma_i^{\beta}/(\alpha+\sigma_i^{\beta\gamma})^{1/\gamma}$, $k < i \leq n+1$; this not only guarantees the filtering of small singular values but also improves the approximation order of solutions. □

4. Stability Analysis of the Proposed Method

Theorem 3. *Suppose that the solution x^+ of $Kx = y$ satisfies $x^+ = (K^*K)^\nu z \in R(K^*K)^\nu$, $z \in X$, and $\|z\| \leq E$; if choosing the regularization parameter $\alpha(\delta) = c(\delta/E)^{\sigma r/(2\nu+1)}$ (c is a positive constant), then there are the following error estimates:*

$$\left\| x^\delta_{\alpha(\delta)} - x^+ \right\| = O\left(\delta^{2\nu/(2\nu+1)}\right). \quad (33)$$

Proof. As we all know, the error estimates of true solution and regular solution can be expressed as follows:

$$\left\| x^\delta_\alpha - x^+ \right\| \leq \left\| R_\alpha \right\| \cdot \delta + \left\| R_\alpha y - x^+ \right\|. \quad (34)$$

It is known from Theorem 2 that we have

$$\left\| R_\alpha \right\| \leq c(\alpha) = \frac{1}{\alpha^{1/\sigma r}} \quad (35)$$

By using the singular system of operator K, then we have

$$\begin{aligned} \left\| R_\alpha y - x^+ \right\|^2 &= \sum_{i=1}^{\infty} \left| q(\alpha,\mu_i) - 1 \right|^2 \cdot \left| (x^+, x_i) \right|^2 \\ &= \sum_{i=1}^{\infty} \left| q(\alpha,\mu_i) - 1 \right|^2 \cdot \left| \left((K^*K)^\nu z, x_i \right) \right|^2 \\ &= \sum_{i=1}^{\infty} \left| q(\alpha,\mu_i) - 1 \right|^2 \cdot \left| \left(\sum_{j=1}^{\infty} \mu_j^{2\nu} (z, x_j) x_j, x_i \right) \right|^2 \\ &= \sum_{i=1}^{\infty} \left| q(\alpha,\mu_i) - 1 \right|^2 \cdot \left| \mu_i^{2\nu} (z, x_i) \right|^2 \\ &= \sum_{i=1}^{\infty} \left| q(\alpha,\mu_i) - 1 \right|^2 \cdot \mu_i^{4\nu} \cdot \left| (z, x_i) \right|^2. \end{aligned} \quad (36)$$

when $\mu^{\sigma r} < \alpha$ and $0 < q(\alpha,\mu) < 1$, such that $|q(\alpha,\mu_i) - 1| < 1$, hence, we can obtain

$$\left| q(\alpha,\mu_i) - 1 \right| \cdot \mu_i^{2\nu} < \mu_i^{2\nu} = \left(\mu_i^{\sigma r}\right)^{2\nu/\sigma r} < \alpha^{2\nu/\sigma r}. \quad (37)$$

When $\mu^{\sigma r} \geq \alpha$ and $q(\alpha,\mu) = 1$, then we have

$$\left| q(\alpha,\mu_i) - 1 \right| \cdot \mu_i^{2\nu} = 0 \cdot \mu_i^{2\nu} = 0 < \alpha^{2\nu/\sigma r}. \quad (38)$$

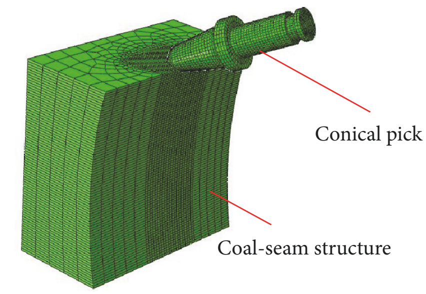

FIGURE 1: The structure diagram of conical pick and coal-seam structure.

And

$$\begin{aligned} \left\| R_\alpha y - x^+ \right\|^2 &< \alpha^{4\nu/\sigma r} \sum_{i=1}^{\infty} \left| (z, x_i) \right|^2 = \alpha^{4\nu/\sigma r} \cdot \|z\|^2 \\ &\leq \alpha^{4\nu/\sigma r} \cdot E^2. \end{aligned} \quad (39)$$

So we can obtain

$$\left\| x^\delta_\alpha - x^+ \right\| \leq \frac{1}{\alpha^{1/\sigma r}} + \alpha^{2\nu/\sigma r} \cdot E. \quad (40)$$

If $\alpha(\delta) = c(\delta/E)^{\sigma r/(2\nu+1)}$, then

$$\begin{aligned} \left\| x^\delta_{\alpha(\delta)} - x^+ \right\| &\leq \delta \cdot \left[c \left(\frac{\delta}{E} \right)^{\sigma r/(2\nu+1)} \right]^{-1/\sigma r} \\ &\quad + \left[c \left(\frac{\delta}{E} \right)^{\sigma r/(2\nu+1)} \right]^{2\nu/\sigma r} \cdot E \\ &= \delta \cdot \left[c^{-1/\sigma r} \left(\frac{\delta}{E} \right)^{-1/(2\nu+1)} \right] \\ &\quad + c^{2\nu/\sigma r} \left(\frac{\delta}{E} \right)^{\sigma r/(2\nu+1)} \cdot E \\ &= \left(c^{-1/\sigma r} + c^{2\nu/\sigma r} \right) \cdot E^{1/(2\nu+1)} \cdot \delta^{2\nu/(2\nu+1)}. \end{aligned} \quad (41)$$

Hence, we can get

$$\left\| x^\delta_{\alpha(\delta)} - x^+ \right\| = O\left(\delta^{2\nu/(2\nu+1)}\right). \quad (42)$$

From the above proofs, we can see that the method proposed in this paper can make the error of the regularization solution reach the asymptotically optimal order. □

5. An Example of Engineering Application

In this section, the proposed method is used to an engineering example of the identification problem of dynamic force acting on conical pick and coal-seam structure.

5.1. The Establishment of Experimental System. The structure diagram of conical pick and coal-seam is made in Figure 1.

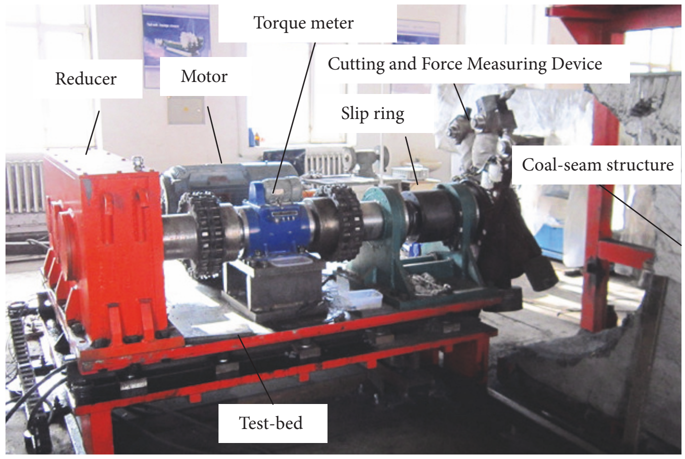

Figure 2: Experimental system.

The parameters are as follows: the coal-seam was 2000 mm × 800 mm × 1750 mm. The density of conical pick and coal-seam is 7800 kg/m^3 and 1607.98 kg/m^3, respectively. The elastic modulus of conical pick and coal-seam is 600 MPa and 322.09 MPa, respectively. The Poisson ratio of conical pick and coal-seam is set as 0.25 and 0.25, respectively [37].

Within our framework, the experimental system was shown in Figure 2. The experimental system includes test-bed, motor, reducer, coupling, cutting mechanism, platform, coal-seam structure, the force-measured device, force sensor, the signal amplifier, and the DaspV10 intelligent data acquisition and signal processing system [38, 39].

5.2. The Principle of Force Measurement. The cutting resistance of the pick when cutting the coal-seam is transmitted through the gear sleeve, and its size is measured by the force sensor at the back end. The force direction of the sensor is defined as the axial load Fz in accordance with the axis of the pick, and the force direction measured is defined as the radial load Fy perpendicular to the axis of the pick.

The force state of the pick in the test force measuring device is shown in Figure 3. Z is the cutting resistance, Y is the propulsion resistance, f is the friction resistance between the support structure and the pick sleeve, beta is the tangential installation angle of the pick, O is the support point of the pick sleeve, l1 is the distance between the tip of the tooth and the support point, and l2 is the distance between the sensor and the support point. According to Figure 3, the force balance and moment balance equations of the pick are obtained.

$$\begin{aligned} Y\cos\beta + Z\sin\beta - f &= F_z \\ (Y\sin\beta - Z\cos\beta)\cdot l_1 + F_y l_2 &= 0 \\ l_1 f &= (l_1 + l_2) f_n F_y \end{aligned} \quad (43)$$

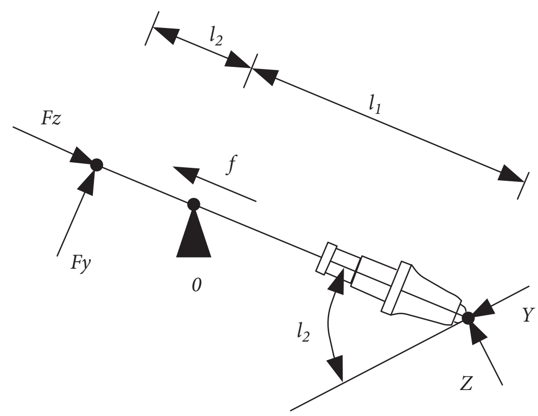

Figure 3: The force diagram of pick.

Setting $k_l = l_2/l_1$, so we have

$$Z = F_z\sin\beta + F_y\left(f_n\sin\beta(1+k_l) + k_l\cos\beta\right). \quad (44)$$

f_n and k_l are called friction coefficient and structural dimension coefficient, respectively.

Experimental conditions: the installation angle of the pick is 45°, the cutting impedance of coal - seam is set to 180 kN/m, the speed of the cutting arm is set to 40.8 r/min, and the traction speed is set to 0.8 m/min. The measured axial and radial loads of the pick are shown in Figures 4(a) and 4(b). According to the load curves of Figures 4(a) and 4(b), the cutting force is converted from (19) at the sampling discrete points, as shown in Figure 4(c), and the measured displacement response is shown in Figure 5.

Under the above experimental conditions, it can be seen that the cutting force obtained by conversion is similar to that of axial load, and the radial load has little effect on its variation. That is to say, the cutting force Z is proportional to the axial load Fz. Therefore, the measured axial load can reflect the size and variation of cutting resistance and can be

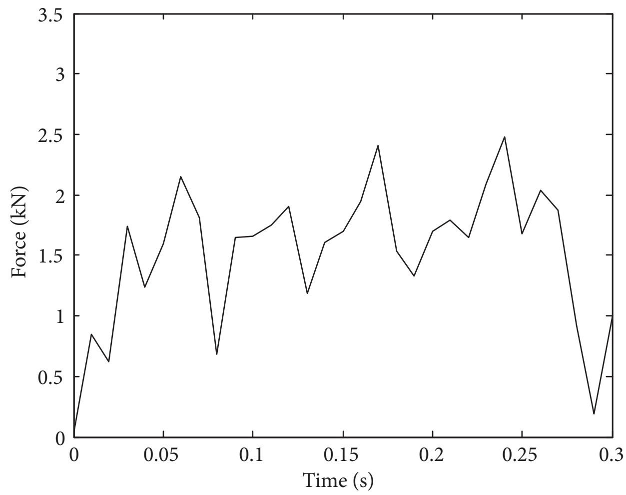

(a) Axial load

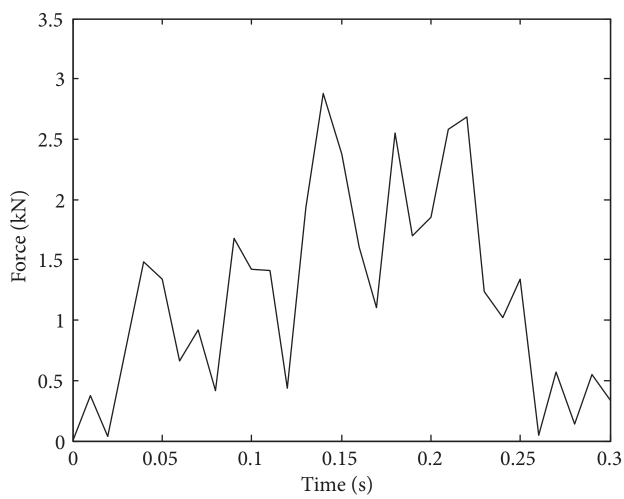

(b) Radial load

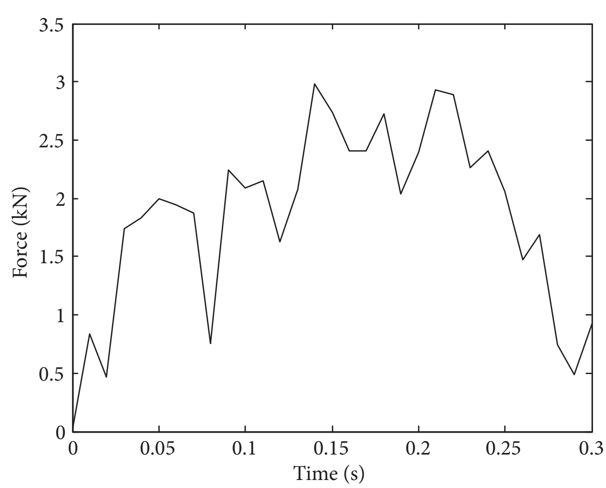

(c) Cutting force

Figure 4: Cutting load and cutting force.

approximately characterized by the measured axial load when analyzing the characteristics of cutting resistance.

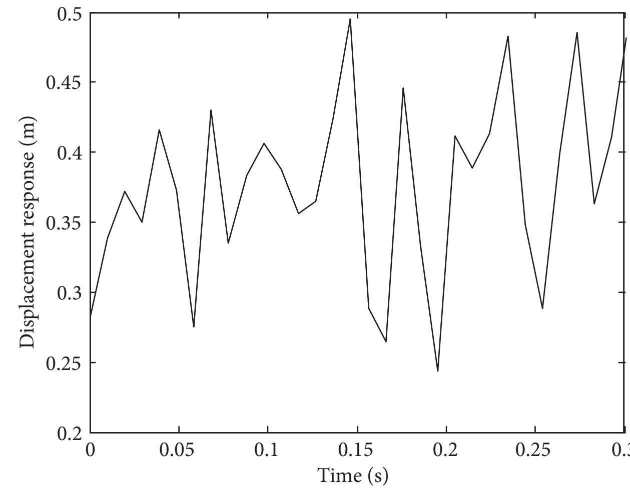

Figure 5: The measured displacement response.

5.3. Result Analysis. Adding a random distributed perturbation to displacement response data, we obtain

$$y^{\delta} = y + \varepsilon \operatorname{randn}\left(\operatorname{size}\left(y\right)\right), \tag{45}$$

where ε indicates the noise level of the measurement displacement response and the randn(•) generates arrays of random numbers whose elements are normally distributed with mean 0, variance $\sigma^2 = 1$, and standard deviation $\sigma = 1$. randn(size(y)) returns an array of random entries that is of the same size as y [40]. The noise level δ can be measured in the sense of root mean square error (RMSE) according to

$$\delta = \left\| y^{\delta} - y \right\|_{l^2} = \left(\frac{1}{N+1} \sum_{i=0}^{N} \left(y - y^{\delta} \right)^2 \right)^{1/2}. \tag{46}$$

This process is known as Morozov's discrepancy principle [41, 42].

Relative error (RE)

$$\mathrm{RE} = \frac{\|\hat{\mathrm{x}} - \mathrm{x}\|}{\|\mathrm{x}\|}. \tag{47}$$

In order to consider the effect of noise level, we set $\varepsilon = 0.01, 0.05, 0.1, 0.20$. All algorithmic programs are set in MATLAB 7.0 and Windows 7 operating system. The identified results of dynamic force are achieved by using different regularization methods in this paper, which are shown in Figures 6, 7, 8, and 9, respectively.

Figures 6(a), 6(b), 6(c), and 6(d) illustrate that the identified force is obtained by adopting various different regularization methods under $\varepsilon = 0.01$, respectively. Figures 7(a), 7(b), 7(c), and 7(d) show the identified force by adopting various different regularization methods under $\varepsilon = 0.05$, respectively. The identified force can be seen from Figures 8(a), 8(b), 8(c), and 8(d), which gives that the identified force under $\varepsilon = 0.10$, and Figures 9(a), 8(b), 8(c), and 9(d) offer the identified force by adopting various different methods under $\varepsilon = 0.20$, respectively.

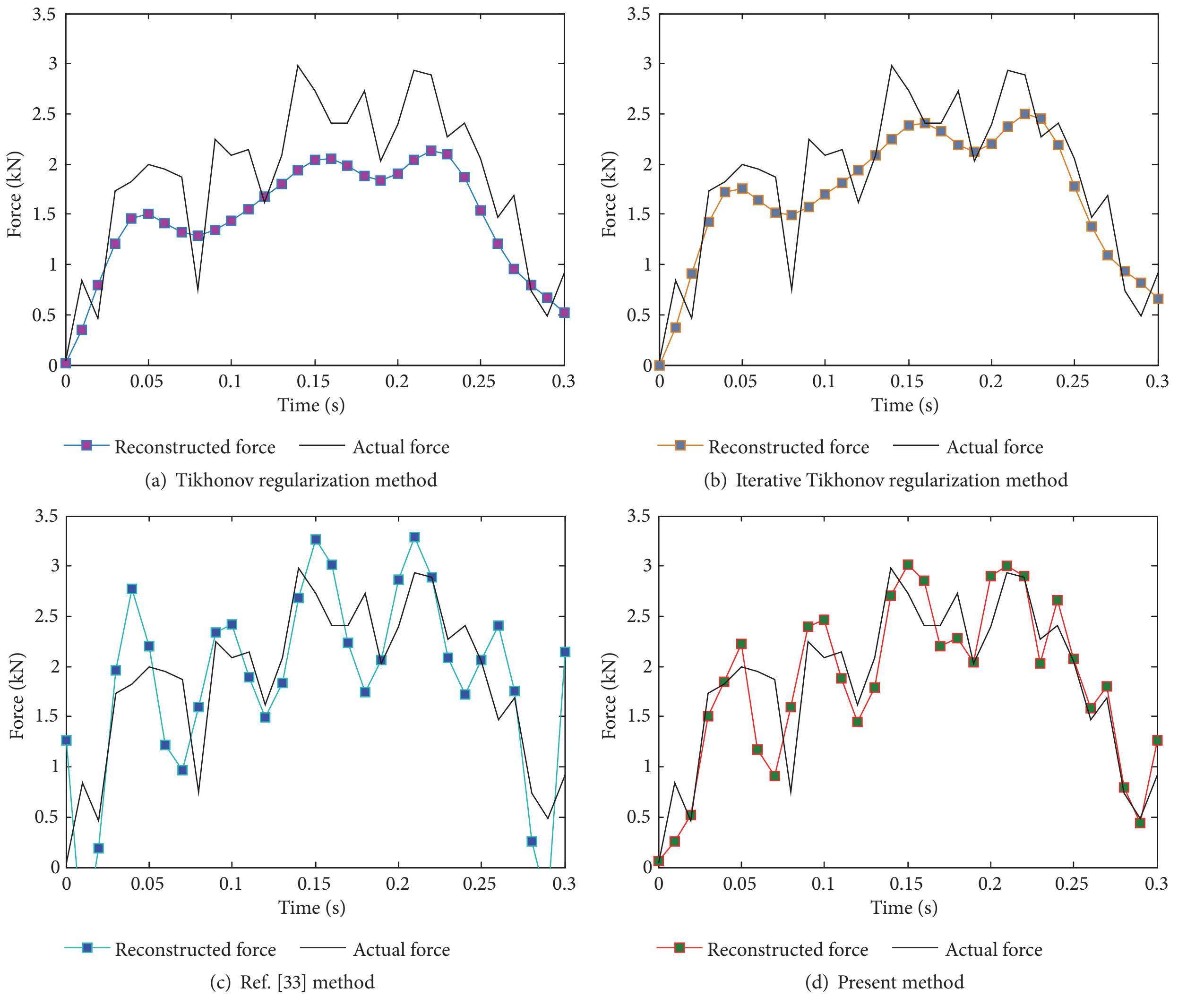

Figure 6: Identified results ($\varepsilon = 0.01$).

Table 1: Analysis of identification results ($\varepsilon = 0.01$).

Evaluation metrics	Tikhonov regularization	Iterative Tikhonov regularization	Ref. [33] method	Present method
RE	0.2719	0.2011	0.1897	0.1832
CC	0.8939	0.9037	0.9145	0.9276
Iterative steps	22	15	10	8

It can be seen from Figures 6, 7, 8, and 9 that the various different methods can identify the dynamic force. On the contrary, the effect of dynamic force identification is different.

To explore the quality of dynamic force identification by adopting various different methods, we give the value of RE and CC and iterative steps, which are shown in Tables 1, 2, 3, and 4. It is easy to see from Table 1 that RE and iterative steps of Figure 6(d) are smaller than that of Figures 6(a), 6(b), and 6(c), On the contrary, CC value presents opposite result. Table 2 shows that RE and iterative steps of Figures 7(a), 7(b), and 7(c) are larger than that of Figure 7(d), and the CC value presents opposite result. Table 3 shows that RE and iterative steps of Figure 8(d) are smaller than that of Figures 8(a), 8(b), and 8(c), but the CC value is the opposite. Table 4 offers that RE and iterative steps of Figure 9(d) are smaller than that of Figures 9(a), 9(b), and 9(c); nevertheless, the CC value presents opposite result.

Hence, compared with the other methods, we find from Tables 1–4 that the proposed method has the smallest RE, the largest CC, and the least iterative steps, so the optimal value is $\varepsilon = 0.01$.

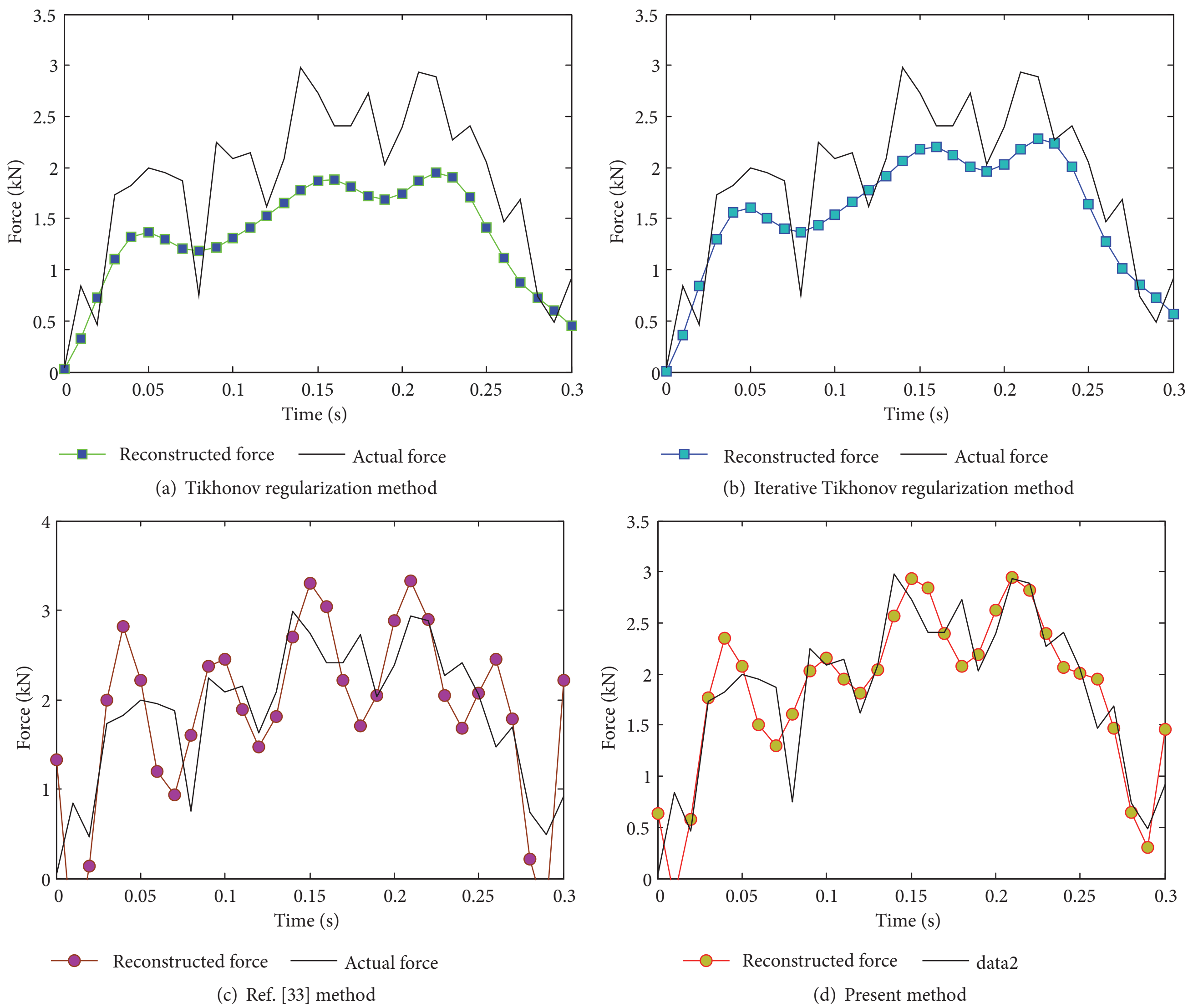

FIGURE 7: Identified results ($\varepsilon = 0.05$).

TABLE 2: Analysis of identification results ($\varepsilon = 0.05$).

Evaluation metrics	Tikhonov regularization	Iterative Tikhonov regularization	Ref. [33] method	Present method
RE	0.3265	0.2327	0.1994	0.1871
CC	0.7940	0.8138	0.9033	0.9104
Iterative steps	30	22	12	9

TABLE 3: Analysis of identification results ($\varepsilon = 0.10$).

Evaluation metrics	Tikhonov regularization	Iterative Tikhonov regularization	Ref. [33] method	Present method
RE	0.3994	0.3011	0.2144	0.1957
CC	0.7291	0.8084	0.8996	0.9001
Iterative steps	37	28	14	10

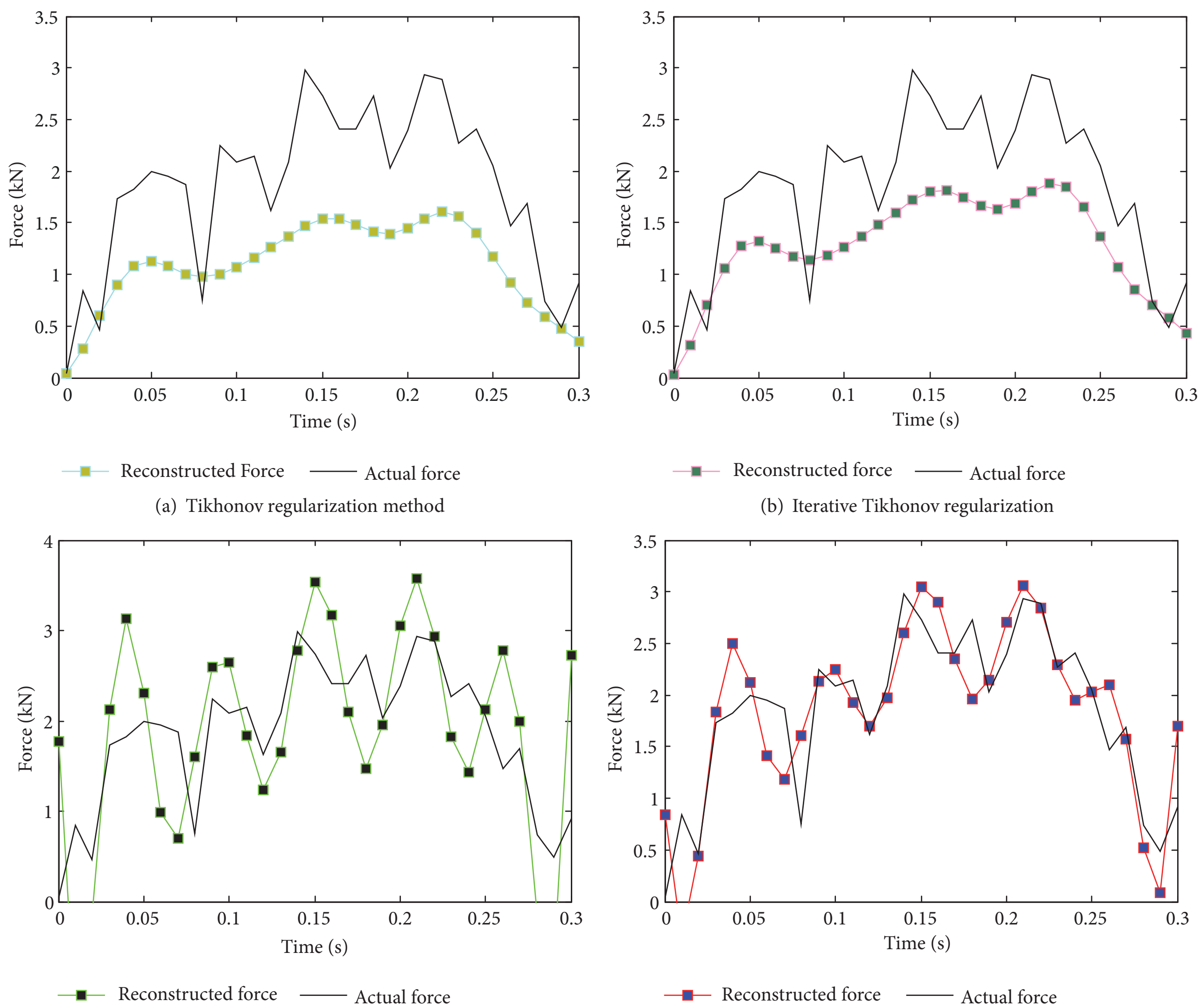

(a) Tikhonov regularization method
(b) Iterative Tikhonov regularization
(c) Reference [33] method
(d) Present method

Figure 8: Identified results ($\varepsilon = 0.10$).

Table 4: Analysis of identification results ($\varepsilon = 0.20$).

Evaluation metrics	Tikhonov regularization	Iterative Tikhonov regularization	Ref. [33] method	Present method
RE	0.5673	0.4033	0.2938	0.2011
CC	0.4497	0.5988	0.8177	0.8846
Iterative steps	50	33	20	13

In addition, with the increase of ε, although RE and iterative steps increase, they do not affect the identification accuracy; that is to say, the small perturbation of the right-hand data will not affect the accuracy of the inversion results, which fully reflects that the present method has a good stability.

Through the analysis, we draw the following conclusions that the present method is successful to identify dynamic force acting on conical pick and coal-seam.

6. Conclusions

In this paper, a novel improved Tikhonov regularization method is proposed to solve the ill-posed problem. Under the current framework, a new regularized filter function is constructed by using the singular system of compact operator, and we prove the stability of the proposed method effectively.

An engineering example indicates that the proposed method has the smallest RE, the largest CC, and the least

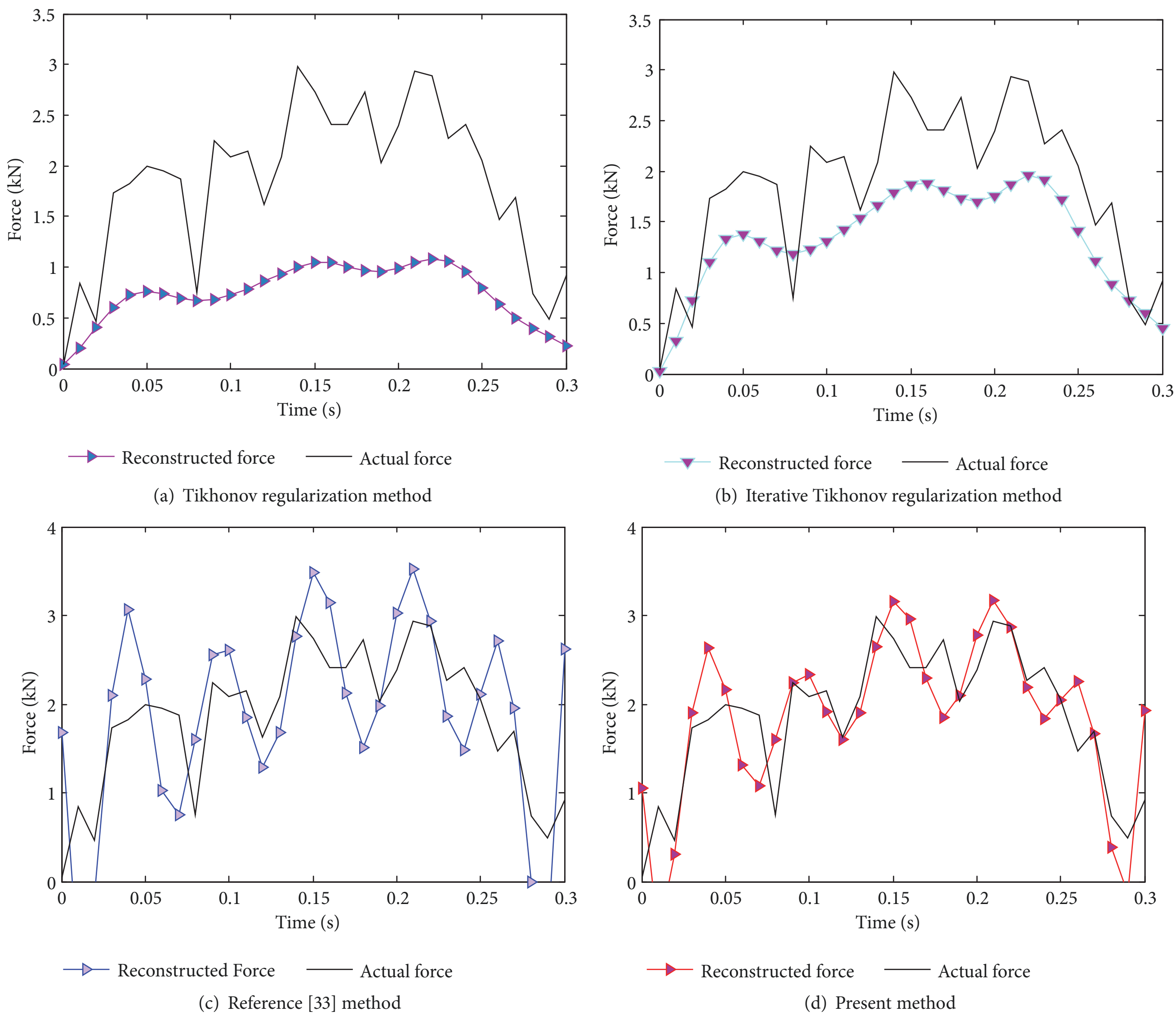

(a) Tikhonov regularization method

(b) Iterative Tikhonov regularization method

(c) Reference [33] method

(d) Present method

Figure 9: Identified results ($\varepsilon = 0.20$).

iterative steps and can obtain an efficient approximation of the actual force compared with the Tikhonov regularization method, iterative Tikhonov regularization method, and Reference [33] method. Meanwhile, the small perturbation of the right-hand data will not affect the accuracy of the inversion results, which fully reflects the present method has a good stability.

Consequently, we can give a new conclusion that the proposed method can offer a unified stable solution for solving the ill-posed problem. Furthermore, we are confident that the proposed method will provide a reference for the next research work.

Data Availability

No data were used to support this study.

Conflicts of Interest

The authors declare that they have no conflicts of interest.

Acknowledgments

This work was supported by the Chinese National Natural Science Foundation (Contract nos. 51674106 and 51274091) and Research and Development of Scientific and Technological Achievements in Provincial Universities of Heilongjiang Education Department (Contract no. TSTAU-C2018005).

References

[1] G. Deschamps and H. Cabayan, "Antenna synthesis and solution of inverse problems by regularization methods," *IEEE Transactions on Antennas and Propagation*, vol. 20, no. 3, pp. 268–274, 1972.

[2] T. S. Jang and S. L. Han, "Numerical experiments on determination of spatially concentrated time-varying loads on a beam: an iterative regularization method," *Journal of Mechanical Science and Technology*, vol. 23, no. 10, pp. 2722–2729, 2009.

[3] T. S. Jang, H. G. Sung, S. L. Han, and S. H. Kwon, "Inverse determination of the loading source of the infinite beam on elastic foundation," *Journal of Mechanical Science & Technology*, vol. 22, no. 12, pp. 2350–2356, 2008.

[4] Karl and C. William, "Feature-preserving regularization method for complex-valued inverse problems with application to coherent imaging," *Optical Engineering*, vol. 45, no. 1, Article ID 017003, 2006.

[5] S. W. Provencher, "A constrained regularization method for inverting data represented by linear algebraic or integral equations," *Computer Physics Communications*, vol. 27, no. 3, pp. 213–227, 1982.

[6] J. M. Varah, "On the numerical solution of ill-conditioned linear systems with applications to ill-posed problems," *SIAM Journal on Numerical Analysis*, vol. 10, no. 2, pp. 257–267, 1973.

[7] X. Jiang and H. Hu, "Reconstruction of distributed dynamic loads on a thin plate via mode-selection and consistent spatial expression," *Journal of Sound and Vibration*, vol. 323, no. 3-5, pp. 626–644, 2009.

[8] L. Wang, X. Han, J. Liu, and J. Chen, "An improved iteration regularization method and application to reconstruction of dynamic loads on a plate," *Journal of Computational and Applied Mathematics*, vol. 235, no. 14, pp. 4083–4094, 2011.

[9] B. Rippey and N. J. Anderson, "Reconstruction of lake phosphorus loading and dynamics using the sedimentary record," *Environmental Science & Technology*, vol. 33, no. 5, pp. 1786–1788, 1996.

[10] F. Liu, H. Li, W. Wang, and B. Liang, "Initial-condition consideration by transferring and loading reconstruction for the dynamic analysis of linear structures in the frequency domain," *Journal of Sound and Vibration*, vol. 336, no. 336, pp. 164–178, 2015.

[11] N. Abu-Shikhah and F. Elkarmi, "Medium-term electric load forecasting using singular value decomposition," *Energy*, vol. 36, no. 7, pp. 4259–4271, 2011.

[12] Y. C. Hon, M. Li, and Y. A. Melnikov, "Inverse source identification by Green's function," *Engineering Analysis with Boundary Elements*, vol. 34, no. 4, pp. 352–358, 2010.

[13] S. Xiang, W. Jiang, and S. Pan, "Sound source identification in a noisy environment based on inverse patch transfer functions with evanescent Green's functions," *Journal of Sound and Vibration*, vol. 359, pp. 68–83, 2015.

[14] H.-H. Chang, "Load identification of non-intrusive load-monitoring system in smart home," *WSEAS Transactions on Systems*, vol. 9, no. 5, pp. 498–510, 2010.

[15] S. Q. Wu, S. S. Law, and Z. Y. Shi, "Moving load and prestress identification using wavelet-based method," *Journal of Applied Mechanics*, vol. 75, no. 2, Article ID 021014, 2008.

[16] W.-M. Li, Z.-H. Jiang, T.-L. Wang, and H.-P. Zhu, "Optimization method based on Generalized pattern search algorithm to identify bridge parameters indirectly by a passing vehicle," *Journal of Sound and Vibration*, vol. 333, no. 2, pp. 364–380, 2014.

[17] A. Cataliotti and V. Cosentino, "Disturbing load identification in power systems: a single-point time-domain method based on IEEE 1459-2000," *IEEE Transactions on Instrumentation and Measurement*, vol. 58, no. 5, pp. 1436–1445, 2009.

[18] D. P. O'Leary and J. A. Simmons, "A bidiagonalization-regularization procedure for large scale discretizations of ill-posed problems," *SIAM Journal on Scientific and Statistical Computing*, vol. 2, no. 4, pp. 474–489, 1981.

[19] U. Tautenhahn and Q. Jin, " Tikhonov regularization and *a posteriori* rules for solving nonlinear ill posed problems ," *Inverse Problems*, vol. 19, no. 1, pp. 1–21, 2003.

[20] B. W. Rust and D. P. O'Leary, "Residual periodograms for choosing regularization parameters for ill-posed problems," *Inverse Problems*, vol. 24, no. 3, p. 034005, 2008.

[21] C. Budd, M. Freitag, and N. Nichols, "Regularization techniques for ill-posed inverse problems in data assimilation," *Computers & Fluids*, vol. 46, no. 1, pp. 168–173, 2011.

[22] L. Dykes and L. Reichel, "On the reduction of Tikhonov minimization problems and the construction of regularization matrices," *Numerical Algorithms*, vol. 60, no. 4, pp. 683–696, 2012.

[23] A. N. Tikhonov, "Solution of incorrectly formulated problems and the regularization method," *Soviet Mathematics - Doklady*, vol. 4, no. 4, pp. 1035–1038, 1963.

[24] C. W. Groetsch, *Inverse Problems in the Mathematical Sciences*, Vieweg, Berlin, Germany, 1993.

[25] D. N. Hào and T. N. Quyen, "Convergence rates for Tikhonov regularization of a two-coefficient identification problem in an elliptic boundary value problem," *Numerische Mathematik*, vol. 120, no. 1, pp. 45–77, 2012.

[26] B. Kaltenbacher, A. Kirchner, and B. Vexler, "Adaptive discretizations for the choice of a Tikhonov regularization parameter in nonlinear inverse problems," *Inverse Problems*, vol. 27, no. 12, p. 125008, 2011.

[27] Z. Bangji, Z. Shouyu, X. Qingxi, and Z. Nong, "Load identification of virtual iteration based on tikhonov regularization and model reduction," *Hunan Daxue Xuebao/Journal of Hunan University Natural Sciences*, vol. 44, no. 2, pp. 53–59, 2017.

[28] H. Ronasi, H. Johansson, and F. Larsson, "A numerical framework for load identification and regularization with application to rolling disc problem," *Computers and Structures*, vol. 89, no. 1-2, pp. 38–47, 2011.

[29] J. Qi-Nian, "Applications of the modified discrepancy principle to tikhonov regularization of nonlinear ill-posed problems," *SIAM Journal on Numerical Analysis*, vol. 36, no. 2, pp. 475–490, 1999.

[30] T. P. Nordberg and I. Gustafsson, "Dynamic regularization of input estimation problems by explicit block inversion," *Computer Methods Applied Mechanics and Engineering*, vol. 195, no. 44-47, pp. 5877–5890, 2006.

[31] P. Kügler and E. Sincich, "Logarithmic convergence rates for the identification of a nonlinear Robin coefficient," *Journal of Mathematical Analysis and Applications*, vol. 359, no. 2, pp. 451–463, 2009.

[32] A. E. Babaev and I. V. Yanchevskii, "Identification of the shock load on an electroelastic bimorph disk," *International Applied Mechanics*, vol. 47, no. 5, pp. 560–566, 2011.

[33] I. Iakovidis and R. M. Gulrajani, "Improving tikhonov regularization with linearly constrained optimization: application to the inverse epicardial potential solution," *Mathematical Biosciences*, vol. 112, no. 1, pp. 55–80, 1992.

[34] C. P. Ren, N. Wang, and C. Liu, "Identification of random dynamic force using an improved maximum entropy regularization combined with a novel conjugate gradient," *Mathematical Problems in Engineering*, vol. 2017, Article ID 9125734, 14 pages, 2017.

[35] A. Kirsch, "An introduction to the mathematical theory of inverse problems," *Applied Mathematics Science*, 1996.

[36] C.-S. Liu, H.-K. Hong, and S. N. Atluri, "Novel algorithms based on the conjugate gradient method for inverting ill-conditioned matrices, and a new regularization method to solve ill-posed linear systems," *Computer Modeling in Engineering & Sciences*, vol. 60, no. 3, pp. 279–308, 2010.

[37] L. Zhang, W. Zhou, and D. H. Li, "A descent modified Polak-Ribiere-Polyak conjugate gradient method and its global convergence," *IMA Journal of Numerical Analysis (IMAJNA)*, vol. 26, no. 4, pp. 629–640, 2006.

[38] C. P. Ren and C. S. Liu, "Experimental research on properties of analog materials of coal and rock," *Journal of Heilongjiang University of Science and Technology*, vol. 24, no. 6, pp. 581–584, 2014.

[39] C.-S. Liu, C.-P. Ren, and D.-G. Li, "Reconstruction and deduction of cutting coal and rock load spectrum on modified discrete regularization algorithm," *Journal of the China Coal Society*, vol. 39, no. 5, pp. 981–986, 2014.

[40] T. Jang, "Non-parametric simultaneous identification of both the nonlinear damping and restoring characteristics of nonlinear systems whose dampings depend on velocity alone," *Mechanical Systems and Signal Processing*, vol. 25, no. 4, pp. 1159–1173, 2011.

[41] T. Jang, H. Baek, H. S. Choi, and S. Lee, "A new method for measuring nonharmonic periodic excitation forces in nonlinear damped systems," *Mechanical Systems and Signal Processing*, vol. 25, no. 6, pp. 2219–2228, 2011.

[42] T. S. Jang, "A method for simultaneous identification of the full nonlinear damping and the phase shift and amplitude of the external harmonic excitation in a forced nonlinear oscillator," *Computers & Structures*, vol. 120, pp. 77–85, 2013.